

IMAGE DENOISING BY SOFT SHRINKAGE IN ADAPTIVE DUAL TREE DISCRETE WAVELET PACKET DOMAIN

V.Saranya^{#1} G.Shobana^{#2} A.Velusamy^{#3}

Abstract - Image Denoising has remained a fundamental problem in the field of image processing. It still remains a challenge for researchers because noise removal introduces artifacts and causes blurring of the images. In the existing system the signal denoising is performed using neighbouring wavelet coefficients. The standard discrete wavelet transform is not shift invariant due to decimation operation. To overcome the problem, signal is transformed to wavelet domain using dual-tree complex wavelet transform which exhibits approximate shift invariance and improved angular resolution. In the proposed system the image denoising is performed using adaptive dual-tree discrete wavelet packets (ADDWP), which is extended from the dual-tree discrete wavelet transform (DDWT) as wavelets give a superior performance in image denoising. With ADDWP, DDWT sub bands are further decomposed into wavelet packets with anisotropic decomposition, so that the resulting wavelets have elongated support regions and more orientations than DDWT wavelets. For denoising the ADDWP coefficients, a statistical model is used to exploit the dependency between real and imaginary parts of the coefficients. Using the statistical model the noise in the image is removed and finally the reconstructed denoised image is achieved.

Keywords : denoising,wavelets, dual-tree, noise, anisotropic decomposition.

I INTRODUCTION

Visual information transmitted in the form of digital images is becoming a major method of communication in the modern age, but the image obtained after transmission is often corrupted with noise. The received image needs processing before it can be used in applications. Image denoising involves the manipulation of the image data to produce a visually high quality image. Digital images play an important role both in daily life applications such as satellite television, magnetic resonance imaging, computer tomography as well as in areas of research and technology such as geographical information systems and astronomy. Data sets collected by image sensors are generally contaminated by noise. Imperfect instruments, problems with the data acquisition process, and interfering natural

phenomena can all degrade the data of interest. Furthermore, noise can be introduced by transmission errors and compression. Thus, denoising is often a necessary and the first step to be taken before the images data is analyzed. It is necessary to apply an efficient denoising technique to compensate for such data corruption. Image denoising still remains a challenge for researchers because noise removal introduces artifacts and causes blurring of the images.

Wavelet-based image denoising algorithms can be generally summarized into three steps: 1) Apply a wavelet transform on the input noisy image; 2) Modify the wavelet coefficients; 3) Apply inverse wavelet transform on the modified coefficients.

II SYSTEM ANALYSIS

The basic idea is the estimation of the uncorrupted image from the distorted or noisy image, and is also referred to as image “denoising”. There are various methods to help restore an image from noisy distortions. Selecting the appropriate method plays a major role in getting the desired image. The denoising methods tend to be problem specific. For example, a method that is used to denoise satellite images may not be suitable for denoising medical images. In order to quantify the performance of the various denoising algorithms, a high quality image is taken and some known noise is added to it. This would then be given as input to the denoising algorithm, which produces an image close to the original high quality image. The performance of each algorithm is compared by computing Peak Signal to Noise Ratio (PSNR) besides the visual interpretation.

ADDITIVE & MULTIPLICATIVE NOISES

In this section the noise commonly present in an image is discussed. Noise is undesired information that contaminates the image. In the image denoising process, information about the type of noise present in the original image plays a significant role. Typical images are corrupted with noise modeled with either a Gaussian, uniform, or salt or pepper distribution. Another typical noise is a speckle noise, which is multiplicative in nature.

Noise is present in an image either in an additive or multiplicative form. An additive noise follows the rule

$$W(x, y) = s(x, y) + n(x, y)$$

While the multiplicative noise satisfies

$$W(x, y) = s(x, y) \times n(x, y)$$

Where $s(x, y)$ is the original signal, $n(x, y)$ denotes the noise introduced into the signal to produce the corrupted image $w(x, y)$, and (x, y) represents the pixel location. The image multiplication means the brightness of the image is varied.

Gaussian noise - This type of noise adds normal distributed noise to the original image. The noise is independent of the image it is applied to. The value of the pixel is altered by the additive Gaussian noise as

$$J(k, l) = x(k, l) + n$$

where n is the noise, $n \sim N(0, v)$, being distributed normally with variance v .

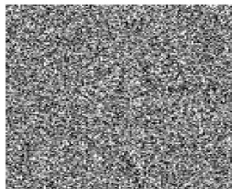


**Fig:2.1 Gaussian noise
(Mean =0, variance 0.05)**

The noisy pixels which are generated anywhere between black and white, distributed according to the Gaussian curve.

Salt and pepper noise – This is the simplest type of noise among all. According to a given density D more or less pixels are flipped randomly to black (0) or white (1). D is just a measure of the amount of noise to be added, not a value. This type of noise is also independent of the image it is applied to.

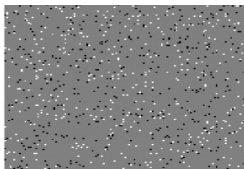


Fig 2.2 Salt and pepper noise

Speckle noise - Speckle adds multiplicative noise to the image according to the following formula:

$$J = I + n * I$$

where n is an array with the size of the original image, filled with random values resulting from a normal distribution (Gaussian distribution) with mean 0 and are controlled by the variance. With this type of noise, noise generation is dependent on the original image, hence the product in the formula. In dark areas (where values are 0 or close to 0) no noise is generated.



Fig 2.3 Speckle noise

III PROPOSED SYSTEM

To estimate an image from a noisy version is a classic problem in image processing. Many promising denoising schemes are based on wavelet transforms. Therefore, there are mainly two avenues to improve denoising performance under the wavelet-based denoising framework: one is to seek more appropriate wavelet transforms and the other is to design better modification strategies for wavelet coefficients. Following the first problem, researchers have successfully boosted denoising performance via directional wavelet transforms. Many directional transforms have been developed under the multiscale analysis framework, including steerable wavelets, wedgelets, dual-tree complex wavelets, curvelets, contourlets, and directionlets. As to the second problem, numerous coefficient modification strategies have been proposed to improve denoising performance. Subband-dependent methods, such as SureShrink and BayesShrink, provide better performance than the uniform thresholding method VisuShrink. Exploiting the dependency between coefficients provides better denoising performance.

DDWT TRANSFORM

DDWT proposed by Kingsbury is one of promising tools with the following three main advantages: direction selectivity, limited redundancy, and shift invariance. The first two features are especially appealing for image coding. Basis functions with direction selectivity can characterize directional structures efficiently. DDWT provides a good solution against the two main drawbacks of the conventional DWT: shift variance and lack of directionality. It is a redundant, non-separable, and complex wavelet transform. There are two DWT decomposition trees for 1-D DDWT: one is for the real part and the other is for the imaginary part. That is why it is named dual-tree.

To achieve shift invariance, the DDWT wavelets are designed to be nearly analytic: the imaginary part is approximately the Hilbert transform of the real part. The analyticity of DDWT not only gives shift invariance, but also brings directionality for 2-D DDWT or higher dimensional DDWT. Being analytic, a 1-D DDWT wavelet has a single-sided spectrum. For a 2-D DDWT wavelet, the spectrum support only lies in one quadrant on the 2-D frequency plane. Since the spectrum of a real function is symmetric with respect to the origin, the spectrum of either the real part or imaginary part is supported only in two diagonal quadrants on the 2-D frequency plane. As a result, both the real and imaginary parts are directional at a certain direction.

DDWT is a complex transform whose wavelet function is restrained to have single-sided spectrum. Either the real part or the imaginary part can be used as a stand-alone transform since they both guarantee perfect reconstruction. Meanwhile, DDWT is an over complete transform with redundancy of 2^m : 1 for m -dimensional signals. Only the real part of DDWT is taken in coding applications to reduce the introduced redundancy.

The implementation of 2-D DDWT consists of two steps. Firstly, an input image is decomposed up to a desired level by two separable 2-D DWT branches, branch a and branch b, whose filters are specifically designed to meet the Hilbert pair requirements. Then six high-pass subbands are generated: HLa, LH_a, HH_a, HL_b, LH_b, and HH_b, at each level. Secondly, every two corresponding subbands which have the same pass-bands are linearly combined by either averaging or differencing. As a result, subbands of 2D DDWT at each level are obtained as $(HL_a + HL_b) / 2$, $(HL_a - HL_b) / 2$, $(LH_a + LH_b) / 2$, $(LH_a - LH_b) / 2$, $(HH_a + HH_b) / 2$ and $(HH_a - HH_b) / 2$.

ANISOTROPIC DECOMPOSITION

In this section, the brief introduction for the anisotropic decomposition on DDWT is given. Then, the greedy basis selection algorithm is developed to select the decomposition structure. The extension from dyadic decomposition to anisotropic decomposition of wavelet packets shows better adaptability to the features of images.

In anisotropic decomposition, subbands are allowed to be only decomposed vertically or horizontally rather than along both directions sequentially. In this way, anisotropic wavelet packets based on DWT provides basis functions with different aspect ratios which are thus anisotropic. However, the directions of these basis functions are still only horizontal, vertical, or diagonal. Noting that DDWT subbands are directional, incorporating anisotropic decomposition into DDWT (ADDWT) will generate anisotropic yet directional basis functions. For example, performing vertical decomposition on the 1st subband will produce two new subbands. The resulting basis functions and corresponding idealized spectrum supports are illustrated. It can be observed that the resulting basis functions are indeed anisotropic and directional.

Different decomposition strategies would generate different basis functions. Naturally, one would like to select basis functions that best adapt to the regarding image as in DWT-based anisotropic wavelet packet. The computation complexity will increase dramatically if these two stages are jointly optimized.

The isotropic wavelet packet is a quad tree like structure which performs row and column decompositions consecutively in one step. Since row and column decompositions respectively express the vertical and horizontal discontinuity, this structure seems cumbersome when dealing with some images where a prevalent directionality exists in certain subbands. By enabling an arbitrary order of row and column decomposition, the 2-D anisotropic wavelet packets is formed.

In anisotropic wavelet packets, row decomposition is not necessarily followed by column decomposition. Rather, for each step, either a row or column decomposition will be chosen. In this way, it is possible to have the case of several consecutive column decompositions or any combination of row and column decompositions.

Two-dimensional row (column) decomposition divides only

the row (column) space in the tensor product expression of 2-D space. And for several steps of space decomposition, any combination of row and column decompositions can be obtained. This actually increases the flexibility of space decomposition, compared to the 2-D isotropic wavelet packets, where row decomposition is always followed by column decomposition. The selection of row or column decomposition is made for the first step and then for other steps. Both row and column decomposition in the first step can lead to 2-D isotropic wavelet packet decomposition in the second step. Therefore the isotropic wavelet packets are just special cases of anisotropic wavelet packets.

Each step of decomposition corresponds to a 2-D row (column) wavelet transform which takes 1 D discrete wavelet transform along rows (columns). Given an input matrix with size $M \times N$, the row transform yields two coefficient matrices with size $M \times N/2$ each, one for approximation subspace and one for detail subspace, while the column transform yields another two coefficient matrices with size $M/2 \times N$ each, also one for approximation subspace and one for detail subspace. The 2-D row (column) decomposition is the counterpart of 2-D row (column) wavelet transform in the space decomposition sense. The structure for anisotropic wavelet packets is a binary-tree like structure, instead of the quad tree structure in isotropic case. Each node is assigned a value from the value set {row, col, null}, standing for a row decomposition, column decomposition or no decomposition at all in a certain tree branch. Note that the level of the tree cannot exceed $2L$ for an image with size $2^L \times 2^L$.

PROPOSED ALGORITHM

Step 1: Input a Grayscale image.

Step 2: Adding Gaussian noise to the input grayscale image.

Step3: Dual Tree Discrete Wavelet Transformation is applied on input image which is in time domain to convert it into the wavelet domain.

Step 4: Anisotropic wavelet packet decomposition is applied on each DDWT subband, generating directional wavelets of elongated support regions.

Step 5: Greedy Basis selection algorithm is used to select the decomposition structure.

Step 6: Estimating the noise variance σ_n for each wavelet packet with the formula,

$$\sigma_n = \text{median}(|\text{Re}(y_i)|) / 0.6745$$

Step 7: Signal Variance is estimated using the formula,

$$\sigma_u = \sqrt{\text{soft}(\sigma_a^2, \sigma_n^2)}$$

where σ_a^2 is the estimated local variance and σ_n^2 is the estimated noise variance.

Step 8: Calculating Threshold with the help of formula,

$$T = \sqrt{3\sigma_n^2/\sigma}$$

where σ_n^2 is the estimated noise variance and σ is the estimated signal variance.

Step 9: Modifying the wavelet coefficients according to the threshold value. The soft shrinkage function used here is, $u_i = \text{soft}(\sqrt{a_i^2+b_i^2}, \sqrt{3\sigma_n^2/\sigma}) a_i / (\sqrt{a_i^2+b_i^2})$

$$v_i = \text{soft}(\sqrt{a_i^2 + b_i^2}, \sqrt{3\sigma_n^2}/\sigma) b_i / (\sqrt{a_i^2 + b_i^2})$$

$$\text{Soft}(x, T) = \text{sign}(x) \cdot \max(|x| - T, 0)$$

where u_i and v_i forms the real and imaginary part of the denoised wavelet packets.

Step 10: Obtaining the denoised image by applying inverse ADDWP on the thresholded coefficients

GREEDY BASIS SELECTION ALGORITHM

Step 1: Denote α as the coefficients of the current subband, α_{ver}^l and α_{ver}^h the coefficients of the two resulting sub band of vertical decomposition, respectively, α_{hor}^l and α_{hor}^h those of horizontal decomposition.

Step 2: Finding the cost using formula,

$$C_{null} = \|\alpha\|_1$$

$$C_{ver} = \|\alpha_{ver}^l\|_1 + \|\alpha_{ver}^h\|_1$$

$$C_{hor} = \|\alpha_{hor}^l\|_1 + \|\alpha_{hor}^h\|_1$$

where C_{null} defines cost for no decomposition, vertical decomposition C_{ver} , and horizontal decomposition C_{hor} .

Step 3: The decomposition decision for the current subband is determined as

$$\tilde{o} = \arg \min_{o \in D} (C_o)$$

where $D = \{null, ver, hor\}$ is the set of three decomposition decisions, and $null$, ver , and hor stand for no decomposition, vertical decomposition, and horizontal decomposition, respectively

Step 4: If \tilde{o} equals to $null$, then do not perform further decomposition on the current subband; if \tilde{o} equals to ver , then perform vertical decomposition; otherwise perform horizontal decomposition.

Step 5: The same procedure is applied to the resulting subbands, if any, until reaching the maximum level.

LOADING AN IMAGE FOR DENOISING

In this first module an image which is to be denoised is loaded. In real time this image is taken for other modules and here to this original image Gaussian noise is added in the next module.



Fig 3.1 Original clean image

ADDING GAUSSIAN NOISE

To the original clean image additive Gaussian noise is added. A basic and generally accepted model for thermal noise in communication channels, is the set of assumptions that

- The noise is additive, i.e., the received signal equals the transmit signal plus some noise, where the noise is statistically independent of the signal

- The noise is white, i.e., the power spectral density is flat, so the autocorrelation of the noise in time domain is zero for any non-zero time offset

- The noise samples have a Gaussian distribution
 Mostly it is also assumed that the channel is Linear and Time Invariant. The most basic results further assume that it is also frequency non-selective.

Additive White Gaussian Noise (AWGN) is the statistically random radio noise characterized by a wide frequency range with regards to a signal in a communications channel. The noise added to the image will vary from noise variance 10 to 30. Based on the variance the denoising performance will vary.



Fig 3.2 Noise added image

TAKING DUAL TREE DISCRETE WAVELET TRANSFORM

The noisy image is taken for further process. Now the image is in time domain and for further processing it is transformed to wavelet domain using dual tree discrete wavelet transform (DDWT). In one level of transformation DDWT yields twelve subbands with six real parts and six imaginary parts. Here four levels of transformations are taken as it yields better result. So totally this transformation yields 48 sub bands. For first level of decomposition farras filter and for remaining levels Q shift filters are used.



2D DDWT wavelets, the real parts of DDWT wavelets are on the top row while the imaginary parts are on the bottom row



Fig 3.3 Reconstructed image after 2D DDWT

The 2D DDWT wavelets of one level of decomposition. The reconstructed image after four levels of transform. Here visually it can be seen that there is no loss of data between the noisy image and the reconstructed image which shows that the transformation process and the levels taken is good.

TAKING ANISOTROPIC DECOMPOSITION

To the wavelet subbands formed from DDWT transformation anisotropic decomposition is taken. This decomposition transforms the sub bands into wavelet packets. The decomposition structure is chosen adaptively by the greedy algorithm. These wavelet packets are used for further processing. Due to anisotropic decomposition a subband is either decomposed vertically or horizontally. For anisotropic decomposition CDF 9/7 filters are used.

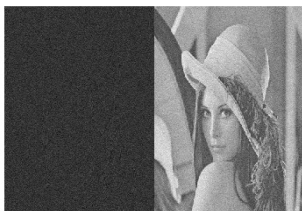


Fig 3.3 Anisotropic decomposition (horizontal decomposition)



Fig 3.4 Anisotropic decomposition (vertical decomposition)

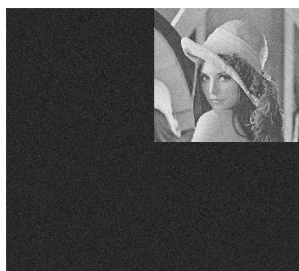


Fig 3.5 Conventional wavelet packet decomposition

The packet from conventional wavelet decomposition; here the wavelet subbands are decomposed both vertically



Fig 3.6 Reconstructed image after anisotropic decomposition

After the decomposition of all the subbands the reconstructed and the original noisy image which shows that there is no loss of data due to decomposition.

ESTIMATING THE NOISE VARIANCE

For denoising the noise variance is calculated for each wavelet packet and used.

The noise variance is calculated using the formula,

$$\sigma_n = \text{median}(|\text{Re}(y_i)|) / 0.6745$$

where $y_i \rightarrow$ ADDWP subband

ESTIMATING THE SIGNAL VARIANCE

Here the signal variance is estimated from the neighborhood. To estimate the signal variance first the local variance of the noisy coefficients is calculated using the formula,

$$\sigma_a^2 = 1/N(\sum_{ai} N_i a_i^2)$$

where N_i contains N coefficients

The neighborhood used here is a square window with the current coefficients at its center. The window size chosen here is 5×5 as it gives a good tradeoff as compared to other window sizes. From the observation model the signal variance is estimated using the formula,

$$\sigma_u = \sqrt{\text{soft}(\sigma_a^2, \sigma_n^2)}$$

where σ_a^2 is the estimated local variance and σ_n^2 is the estimated noise variance.

The local variance and the signal variance is calculated separately for real and imaginary coefficients and then the threshold is also calculated separately for both and then the minimum of both is taken for soft shrinkage function. The threshold is calculated from signal variance using the formula,

$$T = \sqrt{3\sigma_n^2}/\sigma$$

where σ_n^2 is the estimated noise variance and σ is the estimated signal variance.

MODIFYING WAVELET COEFFICIENTS USING SOFT SHRINKAGE

With the threshold value found using the previous module the soft shrinkage function for performing the denoising is formed. This function is applied for each and every wavelet packet. The wavelet coefficients get modified based on the threshold value. The soft shrinkage function used here is,

$$u_i = \text{soft}(\sqrt{a_i^2+b_i^2}, \sqrt{3\sigma_n^2}/\sigma) a_i / (\sqrt{a_i^2+b_i^2})$$

$$v_i = \text{soft}(\sqrt{a_i^2+b_i^2}, \sqrt{3\sigma_n^2}/\sigma) b_i / (\sqrt{a_i^2+b_i^2})$$

$$\text{Soft}(x,T) = \text{sign}(x) \cdot \max(|x| - T, 0)$$

where u_i and v_i forms the real and imaginary part of the denoised wavelet packets.

TAKING INVERSE TRANSFORM

After performing the denoising operation by modifying the wavelet coefficients the inverse transform of anisotropic decomposition and dual tree discrete wavelet transform is taken respectively to get the reconstructed denoised image.



Fig 4.1 Reconstructed denoised image

The above figure shows how well the noise is removed from the image.

IV EXPERIMENTAL RESULTS

The quality of denoising performance is analyzed by calculating the PSNR value of the noisy image and the denoised image. The PSNR value will vary according to the variance of noise added to the image PSNR defines the ratio between the maximum possible power of a signal and the power of corrupting noise that affects the fidelity of its representation. Because many signals have a very wide dynamic range, PSNR is usually expressed in terms of the logarithmic decibel scale. PSNR is most commonly used to measure the quality of reconstruction of lossy compression codecs (e.g., for image compression). The signal in this case is the original data, and the noise is the error introduced by compression. When comparing compression codecs, PSNR is an approximation to human perception of reconstruction quality. Although a higher PSNR generally indicates that the reconstruction is of higher quality, in some cases the reverse may be true.

Tested image

σ_n	PSNR of Noisy image in dB	PSNR of Denoised image in dB
10	28.1445	34.4634
15	24.6514	32.7176
20	22.1626	31.3292
25	20.1916	30.3716
30	18.6466	29.5582

- Image format- Bitmap image (.bmp)
- Image size - 256 * 256 pixels

The above table shows the denoising results for the Lena image. For each noise variance the denoising performance varies and for higher the noise variance added the PSNR value of the denoised image gets decreased .

The graph shows the experimental results for three images Lena, Barbara and Boat which is represented using top, bottom and middle lines respectively. The result shows that the denoising performance is higher for Lena image when compared to Barbara and Boat images. The graph also shows that as the noise variance added to the image gets increased the PSNR value of the denoised image gets decreased.

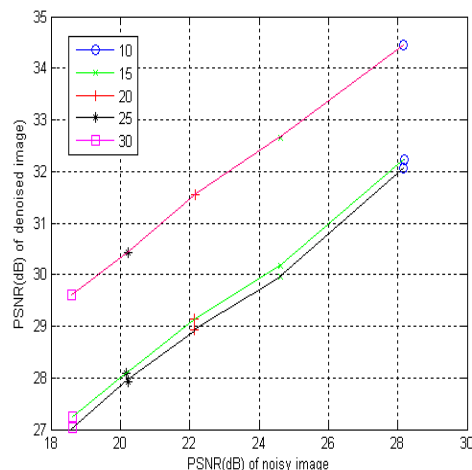


Image denoising results with different noise variances

V CONCLUSION

Thus the soft thresholding method gives a good trade off in image denoising where the denoising is performed using ADDWP coefficients, which extends DDWT to adaptive wavelet packets. In ADDWP, anisotropic decomposition is performed on each DDWT subband, producing directional wavelets of elongated support regions and increasing the number of wavelet orientations. A greedy basis selection algorithm is employed to select wavelet packets to adapt to image denoising. The greedy basis selection shows equal effectiveness (in terms of denoising results) while significantly reducing the computational complexity. The experimental results show that 2-D ADDWP can capture more directional features than 2-D DDWT with the same number of largest coefficients. For denoising, a statistical model is used to exploit the dependency between the real and imaginary parts of ADDWP coefficients. The estimated local variance was used in the shrinkage function to adapt the non stationary characteristics of wavelet coefficients. The above mentioned method produces visually appealing quality due to the usage of 2-D ADDWP.

REFERENCES

[1] Jingyu Yang, Yao Wang, Wenli Xu and Qionghai Dai (2009) 'Image and Video Denoising Using Adaptive Dual-tree Discrete Wavelet Packets', IEEE Transactions on Circuits and Video Technology, VOL. 19, NO. 5, pp.642-655.

[2] Jingyu Yang, Yao Wang, Wenli Xu and Qionghai Dai (2008) 'Image Coding using dual-tree discrete wavelet transform', IEEE Transactions on Image processing, VOL. 17, NO. 9, pp.1555-1566.

[3] Rade Kutil and Dominik Engel (2008) 'Methods for the Anisotropic Wavelet Packet Transform', Applied and Computational Harmonic Analysis, 25(3):295-314.

[4] C.O.S Sorzano, E.Ortiz, M.Lopez, J.Rodrigo (2006) 'Improved bayesian image denoising based on wavelets with applications to electron microscopy', IEEE Transactions on Pattern Recognition, vol. 39, pp.205 - 1213

[5]Jingyu Yang, Jizheng Xu, Feng Wu, Qionghai Dai and Yao Wang (2007) 'Image Coding using 2-D Anisotropic Dual-Tree Discrete Wavelet Transform', IEEE Transactions on Image Processing.

[6]G. Y. Chen, T. D. Bui and A. Krzyzak (2004) 'Image Denoising using Neighbouring wavelet coefficients', IEEE International conference on Image processing.

[7] Wilfred L. Rosenbaum ,HYPERLINK

"http://profiles.spiedigitallibrary.org/summary.aspx?DOI=10.1117%2f12.387655&Name=M.+Stella+Atkins"
M. Stella Atkins HYPERLINK
"http://profiles.spiedigitallibrary.org/summary.aspx?DOI=10.1117%2f12.387655&Name=Gordon+E.+Sarty"and HYPERLINK
"http://profiles.spiedigitallibrary.org/summary.aspx?DOI=10.1117%2f12.387655&Name=Gordon+E.+Sarty"Gordon E. Sarty (2006) 'Classification and performance of denoising algorithms for low signal-to-noise ratio magnetic resonance images', in Proc. SPIE Conf. Wavelets X, San Diego, CA.

[8] Ivan W. Selesnick, Richard G. Baraniuk, and Nick G.Kingsbury (2005) 'The Dual-Tree Complex Wavelet aTransform', IEEE Signal Processing Magazine.

[9]V.sterla and c.heil (2005) 'The Applicaton of multiwavelet filter banks to image processing', IEEE Transactions on signal Processing.

[10] Byung-Jun Yoon, Vaidyanathan.HYPERLINK
"http://ieeexplore.ieee.org/search/searchresult.jsp?searchWithin=p_Authors:.QT.Vaidyanathan,%20P.P..QT.&searchWithin=p_Author_Ids:37272022900&newsearch=true"P.P. (2004) 'Wavelet-based denoising by customized thresholding', Acoustics, Speech, and Signal Processing.

[11] S. Grace Chang, Bin yu and martin vetterli (2000) 'adaptive wavelet thresholding for image denoising and compression', IEEE Transactions on Image Processing.

[12]Alle Meiji and Jos B.T.M Roerdink (2004) 'Denoising functional MR Images-a comparison of wavelet denoising and Gaussian smoothing' , IEEE Transactions on Medical Imaging, Vol.23,no.3

[13] Dan Xu and Minh N.Do (2003) 'Anisotropic 2-D Wavelet Packets and Rectangular Tiling: Theory and Algorithms', in Proc. SPIE Conf. Wavelets X, San Diego, CA.